Biochemical and Biophysical Research Communications 464 (2015) 275–280

Contents lists available at ScienceDirect

Biochemical and Biophysical Research Communications

journal homepage: www.elsevier.com/locate/ybbrc

Inhibition of invasion by glycogen synthase kinase-3 beta inhibitors through dysregulation of actin re-organisation via down-regulation of WAVE2

Yuki Yoshino [a], Manami Suzuki [a], Hidekazu Takahashi [a], Chikashi Ishioka [a, b, *]

[a] Department of Clinical Oncology, Institute of Development, Aging and Cancer, Tohoku University, Seiryo-machi 4-1, Aoba-ku, Sendai 980-8575, Japan
[b] Department of Medical Oncology, Tohoku University Hospital, Tohoku University, Seiryo-machi 1-1, Aoba-ku, Sendai 980-8574, Japan

ARTICLE INFO

Article history:
Received 11 June 2015
Accepted 22 June 2015
Available online 24 June 2015

Keywords:
GSK-3β
WAVE2
Actin cytoskeleton
Focal adhesion

ABSTRACT

Cancer cell invasion is a critical phenomenon in cancer pathogenesis. Glycogen synthase kinase-3β (GSK-3β) has been reported to regulate cancer cell invasion both negatively and positively. Thus, the net effect of GSK-3β on invasion is unclear. In this report, we showed that GSK-3β inhibitors induced dysregulation of the actin cytoskeleton and functional insufficiency of focal adhesion, which resulted in suppressed invasion. In addition, WAVE2, an essential molecule for actin fibre branching, was down-regulated after GSK-3β inhibition. Collectively, we propose that the WAVE2-actin cytoskeleton axis is an important target of GSK-3β inhibitors in cancer cell invasion.

1. Introduction

Glycogen synthase kinase-3 beta (GSK-3β) is a serine/threonine kinase that regulates a wide range of cellular functions [1]. Considering the diversity of its substrates, GSK-3β seems to have a bivalent role in cancer biology. For example, GSK-3β phosphorylates β-catenin, cyclin D1, c-myc and NF-κB, resulting in inhibition of cell proliferation [1]. On the other hand, GSK-3β is necessary for development of a certain kind of leukaemia [2,3], and GSK-3β inhibition results in cancer cell death [4–7]. These reports suggest that GSK-3β acts both as a suppressor and promoter in oncogenesis.

GSK-3β regulates not only cell proliferation but also migration and invasion activities of cells. Cancer cells lose their intercellular adhesion and migrate through the epithelial mesenchymal transition (EMT) [8]. Several transcription factors, including SNAI1, ZEB1 and TWIST, are known to work during the EMT process [8]. Zhou et al. reported that GSK-3β phosphorylates Snail, promoting its degradation [9]. In their report, Snail overexpression could induce EMT only when GSK-3β was inhibited. On the other hand, several reports have shown that GSK-3β inhibitors suppress invasion by dysregulation of adhesion machinery via RAC1 down-regulation [10,11] or the h-prune mediated pathway [12]. Thus, the net effects of GSK-3β on invasive capacity of tumour cells have not been sufficiently elucidated.

RAC1 is a member of the RAS small GTPase superfamily. RAC1 is known to regulate neural fibre formation, actin cytoskeleton organisation and pseudopod formation [13]. When RAC1 is activated, RAC1 activates several downstream effectors, including PAK1 [14], WAVE2 [15] and IQGAP1 [16]. These effectors regulate cell motility, actin re-organisation and cell-extracellular matrix adhesion. When cells migrate, cells form cellular protrusions called 'ruffles' in which the fibrous actin cytoskeleton forms a mesh-like structure [17,18]. WAVE2 or family member N-WASP is necessary for branching of actin fibres from existing fibres to form a mesh-like structure [15,17]. WAVE2 and N-WASP are activated by RAC1 and CDC42, respectively, and act as a scaffold for actin nucleation complexes from which a new actin fibre sprouts [15].

Several reports showed that GSK-3β inhibitors could inhibit cancer cell invasion *in vitro* and leucocyte migration by down-regulation of RAC1 [10,11]. However, the downstream mediator was not elucidated. In this report, we investigated effects of GSK-3β-specific inhibitors on several aspects of cancer cell invasion

Abbreviations: ARP2/3, actin related protein 2 and 3; CDC42, cell division cycle 42; EMT, epithelial mesenchymal transition; FAK1, focal adhesion kinase 1; GSK-3β, glycogen synthase kinase 3-beta; GSKi26, GSK-3β inhibitor XXVI; IQGAP1, IQ motif containing GTPase activating protein 1; MMP, matrix metalloproteinase; N-WASP, Wiskott–Aldrich syndrome-like; WAVE2, WAS protein family, member 2.

* Corresponding author. Department of Clinical Oncology, Institute of Development, Aging and Cancer, Tohoku University, Seiryo-machi 4-1, Aoba-ku, Sendai 980-8575, Japan.
E-mail address: chikashi@idac.tohoku.ac.jp (C. Ishioka).

http://dx.doi.org/10.1016/j.bbrc.2015.06.142
0006-291X/

in vitro. In addition, we also investigated regulation of WAVE2 and actin fibre disorganisation which impedes cellular movement. We propose disorganisation of the actin cytoskeleton through down-regulation of WAVE2 is an important mechanism inhibiting cancer cell invasion by GSK-3β inhibitors.

2. Materials and methods

2.1. Cell lines and culture

MDA-MB-231 and RKO cell lines were purchased from American Type Culture Collection (Manassas, VA). MDA-MB-231 cells were maintained in RPMI-1640 medium supplemented with 8% foetal bovine serum (FBS; Biowest, Nuaille, France). RKO cells were maintained in D-MEM supplemented with 8% FBS. Cell lines were validated by STR analysis using a GenomeLab™ Human STR Primer Set (Beckman Coulter, Inc., Brea, CA).

2.2. Chemical reagents

AR-A0114418 and GSK-3β inhibitor XXVI (GSKi26) were purchased from Merck KGaA (Darmstadt, Germany). Other chemical reagents were purchased from Wako Pure Chemicals Industries (Osaka, Japan) if not otherwise specified.

2.3. 3-D invasion assay

A BD BioCoat™ Matrigel™ invasion chamber (BD Biosciences, San Jose, CA) was used for the 3-D invasion assay. After treatment with 20 μM AR-A0114418 for 24 h, cells were trypsinised and re-suspended in serum-free medium. In each chamber, 25×10^4 cells were seeded. Chambers were set in wells containing growth medium supplemented with 8% FBS and incubated for 24 h in a CO_2 incubator. After matrices and cells remaining in the chamber were removed by cotton swabs, invaded cells were fixed with 4% paraformaldehyde. Chamber membranes were mounted in Mounting Medium with DAPI (Vector Laboratories, Inc., Burlingame, CA) and observed under a BIOREVO BZ-9000 microscope (Keyence, Osaka, Japan). The average number of five 100 × fields was calculated for each membrane.

2.4. Wound healing assay

Two days before wounding, 15×10^4 cells were seeded in a 24-well plate. The next day, reagents were added at indicated concentrations. After 24 h incubation with reagents, the cell monolayer was wounded by a 200 μl pipette tip. Detached cells were carefully washed out. Fresh complete growth media containing 10 μg/ml mitomycin C was added, and cells were allowed to migrate for 24 h. Then, cells were fixed with 4% paraformaldehyde. After staining with crystal violet, wounds were observed under a Leica DM IL LED microscope (Leica Microsystems, Wetzlar, Germany). The wound area was measured by ImageJ 1.49n (http://imagej.nih.gov/ij/).

2.5. Attachment assay

The attachment assay was performed according to a previous report [19] with minor adjustments. In brief, 1×10^4 cells treated with 20 μM AR-A0114418, 20 μM GSKi26 or DMSO for 24 h were plated in gelatin-coated 6-well plates. After a 1 h (MDA-MB-231 cells) or 2 h (RKO cells) incubation, plates were carefully washed with PBS three times and fixed with 4% paraformaldehyde. After staining with crystal violet, cells attached to the well bottom were counted under a Leica DM IL LED microscope. The average number of five 100 × fields was calculated for each well.

2.6. Gelatin zymography

One day before treatment, 2×10^5 cells were seeded in a 6-well plate. After MDA-MB-231 cells were treated with 20 μM AR-A0114418, 20 μM GSKi26 or DMSO for 24 h, cells were allowed to release matrix metalloproteinases (MMPs) into new serum-free media with or without 100 ng/ml epidermal growth factor (EGF) for 24 h. Then, the media were subjected to quantification. Gelatin zymography was performed according to a previous report [20] with minor adjustments. The loading volume was normalised by the cell count using the crystal violet method [21].

2.7. Fluorescent immunocytostaining

Cells were fixed with 4% paraformaldehyde for 15 min at room temperature. After a 5 min permeabilisation with 0.5% TritonX-100/PBS and 1 h blocking with 3% BSA/PBST, cells were incubated in 3% BSA/PBST containing primary antibodies overnight at 4 °C. After washing, cells were incubated in 3% BSA/PBST containing secondary antibodies conjugated with fluorescent dyes for 1 h at room temperature. For fibrous actin staining, Acti-stain 488 phalloidin (Cytoskeleton, Inc., Denver, CO) was added to the secondary antibody solution. Cells were mounted in Mounting Medium with DAPI and observed under a BIOREVO BZ-9000 microscope. Primary and secondary antibodies used are listed in Supplementary Table S1.

2.8. Western blotting

Cells were lysed with HEPES lysis buffer [25 mM HEPES (pH 7.6), 150 mM NaCl, 1% NP-40, 2% SDS and 10% sucrose] supplemented with protease (Roche, Basel, Switzerland) and phosphatase inhibitor cocktails (5 mM NaF, 200 μM sodium orthovanadate, 1 mM sodium molybdate, 2 mM sodium pyrophosphate and 2 mM disodium β-glycerophosphate). Protein concentrations were determined using OPA reagent (Thermo, Waltham, MA) according to the manufacturer's instructions. Protein samples were separated by SDS-PAGE and subjected to immunoblotting. An Odyssey Infrared Imaging System (LI-COR Biosciences, Lincoln, NE) was used for signal detection. Primary and secondary antibodies used are listed in Supplementary Table S1. ImageJ v1.49n was used for image analysis.

2.9. Statistical analysis

JMP 11 software (SAS Institute Inc., Tokyo, Japan) was used for statistical analysis. Graphs were constructed using Excel 2013 (Microsoft Corporation, Redmond, WA). Statistical comparisons between two different samples were made by two-tailed Welch's test. Comparisons between more than two samples were made by ANOVA. When ANOVA indicated a significant difference, post-hoc comparisons were made by Dunnett's test to calculate p-values. A p-value of <0.05 was considered significant.

3. Results

3.1. GSK-3β inhibition disturbs cancer cell invasion through suppression of migration and attachment

To investigate overall effects of GSK-3β inhibition on cancer cell invasion *in vitro*, 3-D matrix invasion assay using a modified Boyden chamber was used. We chose MDA-MB-231 cells for these experiments because this cell line is highly invasive and widely used in studies of cancer cell invasion. After MDA-MB-231 cells were pre-treated with 20 μM AR-A0114418, a specific inhibitor of GSK-3β, or DMSO for 24 h, cells were seeded in a Boyden chamber

coated with extracellular matrix. It was observed that there were significantly fewer invaded cells after pre-treatment with AR-A0114418 than DMSO (Fig. 1A, B).

To investigate molecular mechanisms underlying the inhibition of cancer cell invasion by AR-A0114418, we examined changes of several cellular functions related to invasion, such as follows: cellular migration, attachment to surfaces of culture vessels and activity of MMPs.

First, to examine cellular migration activity, we utilized the cell monolayer wound healing assay. Cellular migration from the

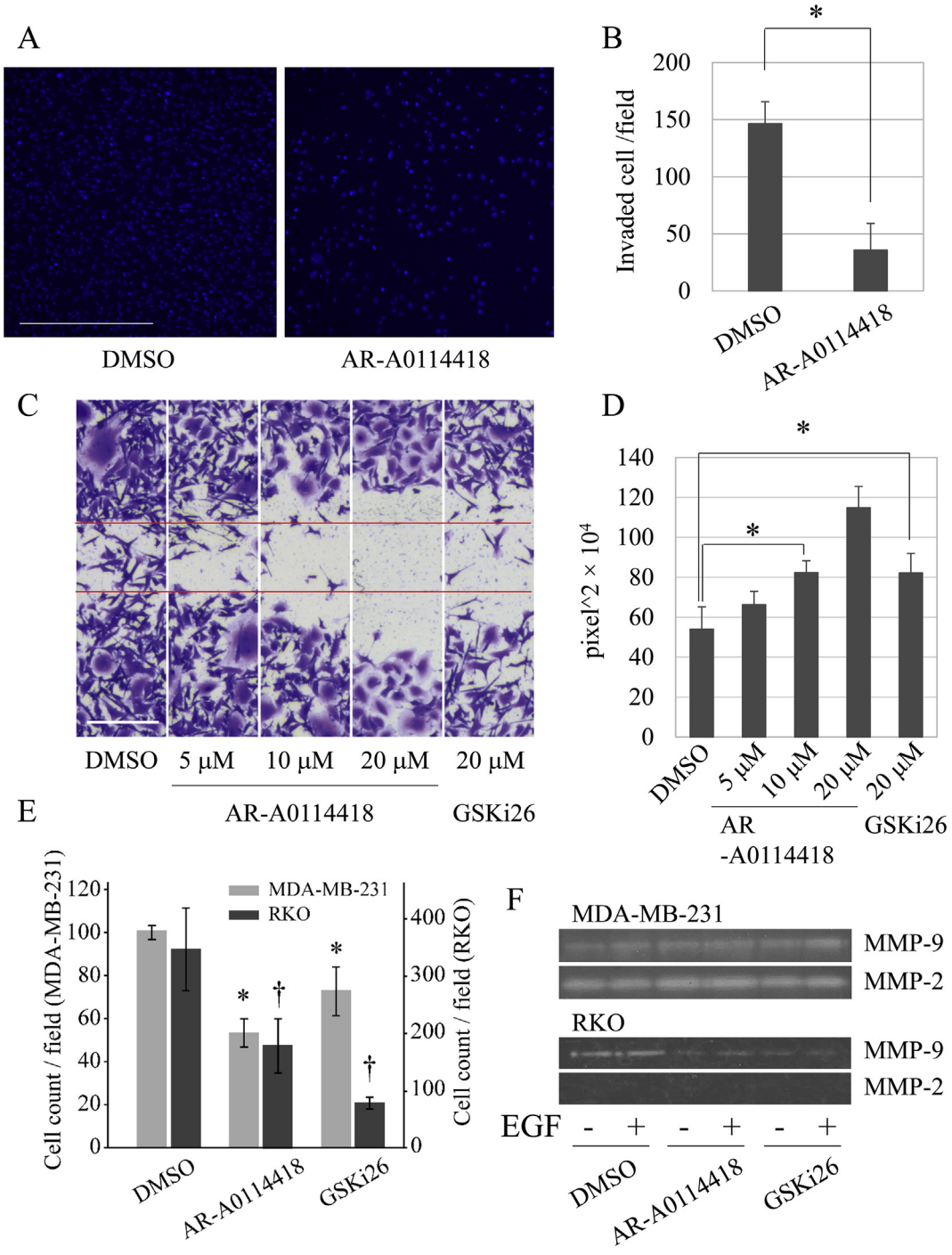

Fig. 1. Effects of GSK-3β inhibitors on cancer cell invasion, migration and attachment. (A) Photographs of invaded cells stained with DAPI (scale bar = 500 μm). (B) Number of invaded cells in samples treated with control (DMSO) or 20 μM AR-A0114418. An average was calculated from cell numbers in five fields of 100 × magnification for each well. Welch's test was performed on triplicates of each sample to calculate p-values. Error bars indicate a 95% confidence interval (CI). (C) Photograph of cell monolayer 24 h after wounding. Before wounding, monolayers were pre-treated with reagents at indicated concentrations. Red lines indicate wound margins of control sample (scale bar = 500 μm). (D) Comparison of remaining wound area after 24 h of migration. Statistical analysis was performed from octuplicate measurements for each treatment. Treatment with either ≥10 μM AR-A0114418 or 20 μM GSKi26 significantly inhibited wound healing. Error bars indicate 95% CI (*$p < 0.0001$). (E) Effect on cellular attachment to culture surfaces. Average number of cells attached to dish bottoms over 1 h (MDA-MB-231 cells) or 2 h (RKO cells) were calculated from counts in five fields of 100 × magnification for each well. Statistical analysis was performed from quadruplicate measurements for each treatment. (*$p < 0.0001$ and †$p < 0.0001$ compared with control). (F) Gelatin zymography of MDA-MB-231 and RKO cells after treatment with DMSO, 20 μM AR-A0114418 or 20 μM GSKi26. After 24 h pre-treatment, cells were allowed to release MMPs into the media for 24 h with or without 100 ng/ml EGF.

wound edge was inhibited by AR-A0114418 in MDA-MB-231 cells (Fig. 1C). The wound area was significantly larger in cells treated with ≥10 μM AR-A0114418 than DMSO (Fig. 1D). In addition, GSKi26 also significantly inhibited migration of cells (Fig. 1C, D). We also confirmed that GSK-3β inhibitors exhibited inhibitory effects on migration of RKO cells (Supplementary Fig. S1A, B), a highly invasive colon cancer cell line.

Second, we investigated the activity of cellular attachment to surfaces of culture vessels. To measure attachment activity, we counted cells attached to gelatin-coated culture dishes 1 or 2 h after seeding. Pre-treatment with AR-A0114418 significantly decreased the number of attached cells compared with DMSO (Fig. 1E). Pre-treatment with GSKi26 also decreased cellular attachment (Fig. 1E). RKO cellular attachment was also significantly inhibited by both GSK-3β inhibitors (Fig. 1E). These data suggested that GSK-3β inhibition suppressed cell-extracellular matrix adhesion activity.

Finally, to measure activities of MMPs, we quantified MMP-2 and MMP-9 by gelatin zymography. Pre-treatment with 20 μM AR-A0114418 or 20 μM GSKi26 did not decrease the activity of either MMP-2 or MMP-9 released into the media from MDA-MB-231 cells (Fig. 1F). In addition, GSK-3β inhibition did not affect the release of MMPs after EGF stimulation (Fig. 1F). Although MMP-2 activity was slightly decreased by both GSK-3β inhibitors in RKO cells, MMP-9 activity was not affected (Fig. 1F). From these data, we believed the effect observed on MMP activity was not sufficient to explain inhibition of invasion by GSK-3β inhibition.

3.2. GSK-3β inhibition disturbs the function rather than the formation of focal adhesion

Cellular attachment to surfaces of culture vessels is maintained by cell-extracellular matrix attachment machinery called focal adhesion [22]; therefore, we examined focal adhesion after GSK-3β inhibition. Immunocytostaining against vinculin revealed that focal adhesion tended to become larger after AR-A0114418 treatment in MDA-MB-231 cells (Fig. 2A). Phospho-FAK staining, another focal adhesion protein, was also enlarged and strengthened after AR-A0114418 treatment (Fig. 2A). Similar results were observed in MDA-MB-231 cells treated with GSKi26 (Supplementary Fig. S2A). This observation was confirmed in RKO cells treated with AR-A0114418 or GSKi26 (Supplementary Fig. S2B).

Next, we aimed to clarify whether enlargement of focal adhesion was due to an acceleration of construction by AR-A0114418. Vinculin-positive spots in MDA-MB-231 cells were decreased after serum starvation (Fig. 2B). When cells were treated with AR-A0114418 under serum-free conditions, vinculin spots did not apparently increase in number, size or brightness (Fig. 2B). In contrast, vinculin spots increased and enlarged when cells were treated with AR-A0114418 in the presence of serum (Fig. 2B). These data suggested that AR-A0114418 itself was not sufficient to accelerate construction of focal adhesion, which was dependent on serum.

3.3. GSK-3β inhibition dysregulates actin fibre organisation

Focal adhesion tethers the intracellular actin cytoskeleton to the extracellular matrix [22]. We investigated changes in the actin cytoskeleton after treatment with GSK-3β inhibitors. Actin formed a fine mesh-like structure in MDA-MB-231 cells treated with DMSO (Fig. 3A). In contrast, actin fibres became denser and tended to make large bundles in the periphery of cells treated with AR-A0114418 (Fig. 3A). GSKi26 also induced a decrease in the actin mesh-like structure and deposition of actin in the periphery of MDA-MB-231 cells (Fig. 3B). Treatment with the two GSK-3β inhibitors did not affect focal adhesion-actin cytoskeleton junctions,

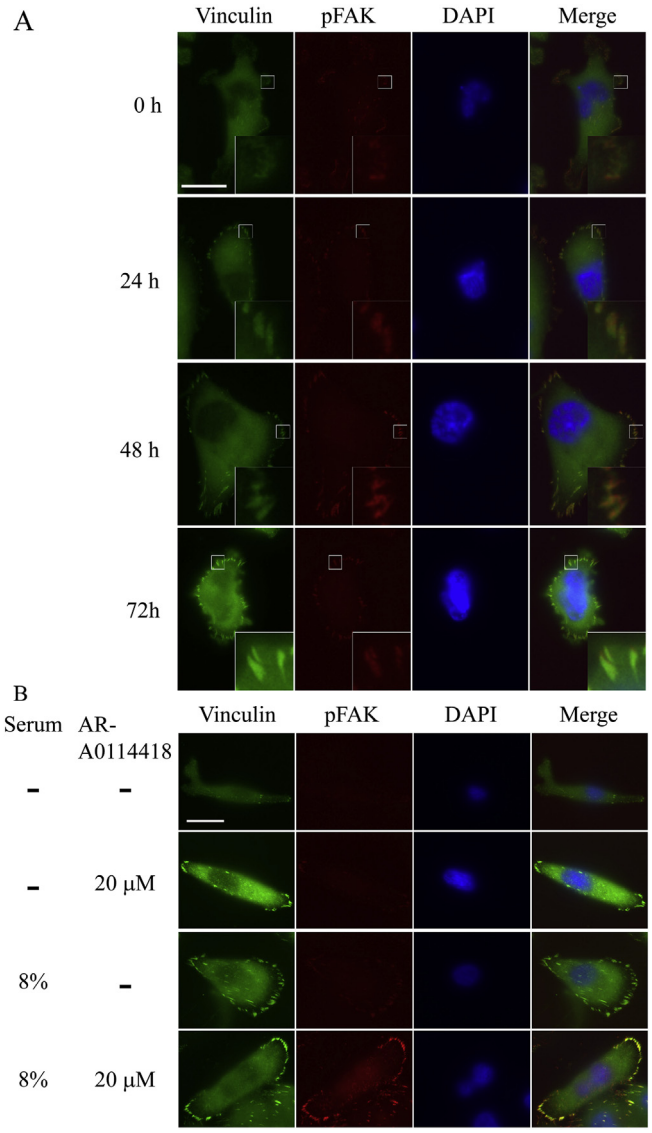

Fig. 2. Enlargement of focal adhesions by GSK-3β inhibition. (A) Changes in focal adhesions by 20 μM AR-A0114418 over time in MDA-MB-231 cells. Inset shows a higher power image indicated by a small white rectangle (scale bar = 20 μm). (B) Serum-dependent construction of focal adhesions in MDA-MB-231 cells. Cells were grown in media containing indicated reagents for 48 h before staining (scale bar = 20 μm).

which were indicated by contact points of fibrous actin and phospho-FAK (Fig. 3A, B). RKO cells had a large number of filopodia, which intermingled with those of neighbouring cells (Supplementary Fig. S3). Because of the intense signal from filopodia, changes in the cytoplasmic actin structure were difficult to assess. Although, actin fibres seemed to lose their cytoplasmic mesh-like structure and have increased intensity in the periphery of RKO cells treated with either GSK-3β inhibitor at higher concentrations (Supplementary Fig. S3).

3.4. Down-regulation of WAVE2 by GSK-3β inhibition impeded actin fibre branching

To investigate the mechanism of dysregulation of the actin cytoskeleton, we examined WASP family proteins WAVE2 and N-WASP. WAVE2 expression was decreased 48 h after addition of 20 μM AR-A0114418 in MDA-MB-231 cells (Fig. 4A). Densitometric

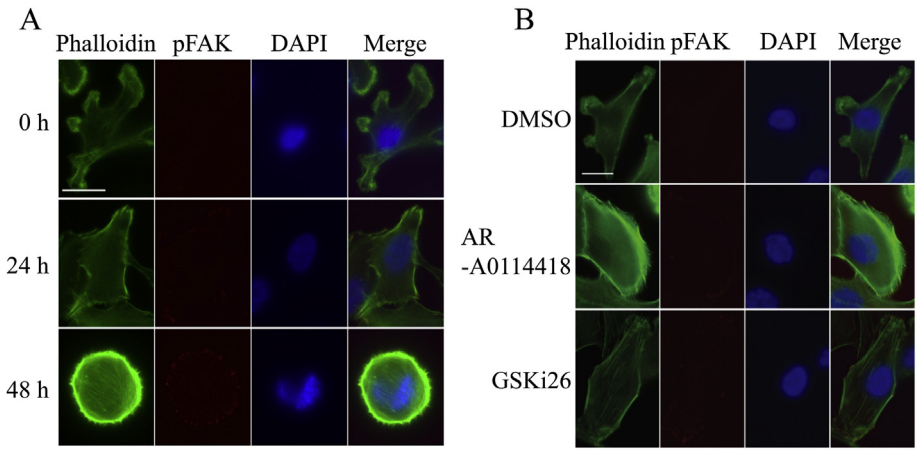

Fig. 3. Actin fibre dysregulation by GSK-3β inhibition. (A) Changes in fibrous actin structure after 20 μM AR-A0114418 treatment over time in MDA-MB-231 cells (scale bar = 20 μm). (B) Fibrous actin structure after incubation with two distinct GSK-3β inhibitors in MDA-MB-231 cells. Cells were treated with DMSO, 20 μM AR-A0114418 or 20 μM GSKi26 for 48 h (scale bar = 20 μm).

analysis showed that WAVE2 expression was significantly lower in AR-A0114418-treated versus DMSO-treated cells (Fig. 4B). GSKi26 also significantly decreased WAVE2 expression in MDA-MB-231 cells (Fig. 4A, B). N-WASP expression was very low in control cells and not apparently affected by treatment with AR-A0114418 or GSKi26 (Fig. 4A). In RKO cells, similar results were observed by treatment with the two GSK-3β inhibitors (Supplementary Fig. S4).

4. Discussion

In this study, we found functional insufficiency of focal adhesion and dysregulation of the actin cytoskeleton were mechanisms inhibiting cancer cell invasion by GSK-3β inhibitors. Focal adhesion was increased and enlarged after GSK-3β inhibition even though cellular attachment to culture vessels was impeded. This suggests functional rather than numerical insufficiency was induced by GSK-3β inhibition. Enlargement of focal adhesion may be a compensatory change following functional insufficiency.

In addition to functional insufficiency of focal adhesion, actin filaments that normally made fine mesh-like structures became large bundle-like structures and deposited in the periphery of cells treated with GSK-3β inhibitors. This suggested that GSK-3β inhibitors suppressed branching of actin filaments. In fact, WAVE2 was down-regulated by GSK-3β inhibitor treatment. Wiskott–Aldrich syndrome proteins, including WAVE2, are necessary for actin branching from existing actin fibres. Therefore, actin fibres could not make a mesh-like structure under GSK-3β inhibition. This actin disorganisation resulted in a decrease in cellular motility.

WAVE2 and N-WASP both belong to the Wiskott–Aldrich syndrome protein family and are activated and stabilized by RAC1 and CDC42, respectively [15]. GSK-3β inhibition has been reported to inhibit RAC1 activation, although the precise mechanism has not yet been elucidated [10,11]. In our experiments, only WAVE2 was decreased by the GSK-3β inhibitors. This result was compatible with past reports that showed RAC1 repression by GSK-3β inhibitors. From these data and past reports, we propose the RAC1/WAVE2/actin cytoskeleton signalling pathway is an effector of GSK-3β in the context of cancer cell invasion.

The actin cytoskeleton is tethered to the extracellular matrix by focal adhesion. Therefore, actin organisation can affect functions of focal adhesion. It is possible that GSK-3β inhibitors impeded cellular adhesion activity through dysregulation of actin

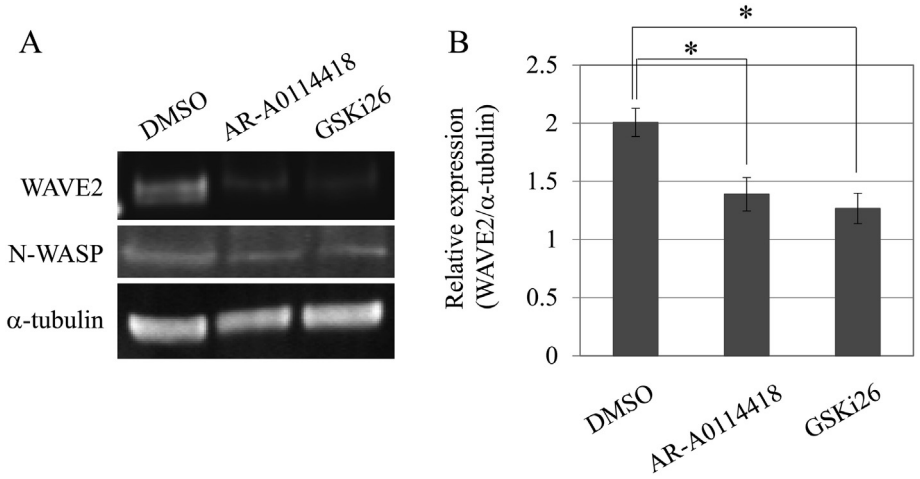

Fig. 4. Down-regulation of WAVE2 by GSK-3β inhibition. (A) Western blot of WAVE2 and N-WASP after 48 h treatment with 20 μM AR-A0114418 or GSKi26. α-tubulin was used as an internal control. (B) WAVE2 protein levels after 48 h treatment with 20 μM AR-A0114418 or 20 μM GSKi26. Protein levels were normalised by α-tubulin expression. Statistical analysis was performed from hexaplicate measurements. Error bars indicate a 95% confidence interval (*$p < 0.0001$).

organisation. If this was the case, down-regulation of the RAC1/WAVE2/actin cytoskeletal axis would induce not only a decrease of cellular motility but also cellular adhesion to surrounding materials. In this study, the direct target of GSK-3β in actin regulation and adhesion machinery was not elucidated. Therefore, whether other small GTPase proteins and Wiskott–Aldrich syndrome protein family members participate should be clarified in future studies.

In conclusion, we identified the RAC1/WAVE2/actin cytoskeletal axis as a potential target signalling pathway of GSK-3β inhibitors in cancer cell invasion. Because this pathway is a downstream effector of EMT, the effects of GSK-3β inhibition should be independent of EMT status. Therefore, inhibition of this pathway may be a useful strategy for inhibiting cancer cell invasion. Future studies are required to further clarify the role of GSK-3β in cancer cell invasion, the mechanisms regulating RAC1 activation and focal adhesion function by GSK-3β.

Financial support

This study was supported in part by the Ministry of Education, Culture, Sports, Science and Technology, Japan.

Conflicts of interest

The authors have no conflicts of interest to disclose.

Author contributions

C.I. supervised the study. Y.Y. and C.I. designed the experiments. Y.Y., M.S., and H.T. performed the experiments. Y.Y. analysed the data. Y.Y and C.I. wrote the manuscript. All authors have reviewed the manuscript.

Acknowledgements

We are sincerely grateful to Professor Akira Horii and Dr. Shinichi Fukushige (Department of Molecular Pathology, School of Medicine, Tohoku University, Miyagi, Japan) and Professor Natsuko Chiba (Department of Cancer Biology, Institute of Development, Aging and Cancer, Tohoku University, Miyagi, Japan) for providing constructive discussions and technical advice.

Appendix A. Supplementary data

Supplementary data related to this article can be found at http://dx.doi.org/10.1016/j.bbrc.2015.06.142.

Transparency document

Transparency document related to this article can be found online at http://dx.doi.org/10.1016/j.bbrc.2015.06.142.

References

[1] U. Maurer, F. Preiss, P. Brauns-Schubert, L. Schlicher, C. Charvet, GSK-3-at the crossroads of cell death and survival, J. Cell. Sci. 127 (2014) 1369–1378, http://dx.doi.org/10.1242/jcs.138057.

[2] Z. Wang, K.S. Smith, M. Murphy, O. Piloto, T.C.P. Somervaille, M.L. Cleary, Glycogen synthase kinase 3 in MLL leukaemia maintenance and targeted therapy, Nature 455 (2008) 1205–1209, http://dx.doi.org/10.1038/nature07284.

[3] J.A. McCubrey, L.S. Steelman, F.E. Bertrand, N.M. Davis, S.L. Abrams, G. Montalto, et al., Multifaceted roles of GSK-3 and Wnt/β-catenin in hematopoiesis and leukemogenesis: opportunities for therapeutic intervention, Leukemia 28 (2014) 15–33, http://dx.doi.org/10.1038/leu.2013.184.

[4] M.R. Mirlashari, I. Randen, J. Kjeldsen-Kragh, Glycogen synthase kinase-3 (GSK-3) inhibition induces apoptosis in leukemic cells through mitochondria-dependent pathway, Leuk. Res. 36 (2012) 499–508, http://dx.doi.org/10.1016/j.leukres.2011.11.013.

[5] A. Shakoori, W. Mai, K. Miyashita, K. Yasumoto, Y. Takahashi, A. Ooi, et al., Inhibition of GSK-3 beta activity attenuates proliferation of human colon cancer cells in rodents, Cancer Sci. 98 (2007) 1388–1393, http://dx.doi.org/10.1111/j.1349-7006.2007.00545.x.

[6] W. Zhou, L. Wang, S.-M. Gou, T.-L. Wang, M. Zhang, T. Liu, et al., ShRNA silencing glycogen synthase kinase-3 beta inhibits tumor growth and angiogenesis in pancreatic cancer, Cancer Lett. 316 (2012) 178–186, http://dx.doi.org/10.1016/j.canlet.2011.10.033.

[7] Q. Zhu, J. Yang, S. Han, J. Liu, J. Holzbeierlein, J.B. Thrasher, et al., Suppression of glycogen synthase kinase 3 activity reduces tumor growth of prostate cancer in vivo, Prostate 71 (2011) 835–845, http://dx.doi.org/10.1002/pros.21300.

[8] K. Steinestel, S. Eder, A.J. Schrader, J. Steinestel, Clinical significance of epithelial-mesenchymal transition, Clin. Transl. Med. 3 (2014) 17, http://dx.doi.org/10.1186/2001-1326-3-17.

[9] B.P. Zhou, J. Deng, W. Xia, J. Xu, Y.M. Li, M. Gunduz, et al., Dual regulation of Snail by GSK-3beta-mediated phosphorylation in control of epithelial-mesenchymal transition, Nat. Cell. Biol. 6 (2004) 931–940, http://dx.doi.org/10.1038/ncb1173.

[10] A. Kitano, T. Shimasaki, Y. Chikano, M. Nakada, M. Hirose, T. Higashi, et al., Aberrant glycogen synthase kinase 3β is involved in Pancreatic cancer cell Invasion and resistance to therapy, PLoS One 8 (2013), http://dx.doi.org/10.1371/journal.pone.0055289.

[11] S. Rom, S. Fan, N. Reichenbach, H. Dykstra, S.H. Ramirez, Y. Persidsky, Glycogen synthase kinase 3?? inhibition prevents monocyte migration across brain endothelial cells via Rac1-GTPase suppression and down-regulation of active integrin conformation, Am. J. Pathol. 181 (2012) 1414–1425, http://dx.doi.org/10.1016/j.ajpath.2012.06.018.

[12] T. Kobayashi, S. Hino, N. Oue, T. Asahara, M. Zollo, W. Yasui, et al., Glycogen synthase kinase 3 and h-prune regulate cell migration by modulating focal adhesions, Mol. Cell Biol. 26 (2006) 898–911, http://dx.doi.org/10.1128/MCB.26.3.898.

[13] A. Sadok, C.J. Marshall, Rho GTPases: masters of cell migration, Small GTPases 5 (2014) e29710, http://dx.doi.org/10.4161/sgtp.29710.

[14] P. Kreis, J.V. Barnier, PAK signalling in neuronal physiology, Cell. Signal 21 (2009) 384–393, http://dx.doi.org/10.1016/j.cellsig.2008.11.001.

[15] T.H. Millard, S.J. Sharp, L.M. Machesky, Signalling to actin assembly via the WASP (Wiskott-Aldrich syndrome protein)-family proteins and the Arp2/3 complex, Biochem. J. 380 (2004) 1–17, http://dx.doi.org/10.1042/BJ20040176.

[16] S. Kuroda, M. Fukata, K. Kobayashi, M. Nakafuku, N. Nomura, A. Iwamatsu, et al., Identification of IQGAP as a putative target for the small GTPases, Cdc42 and Rac1, J. Biol. Chem. 271 (1996) 23363–23367, http://dx.doi.org/10.1074/jbc.271.38.23363.

[17] J.-L. Hoon, W.-K. Wong, C.-G. Koh, Functions and regulation of circular dorsal ruffles, Mol. Cell. Biol. 32 (2012) 4246–4257, http://dx.doi.org/10.1128/MCB.00551-12.

[18] H. Schnittler, M. Taha, M.O. Schnittler, A.A. Taha, N. Lindemann, J. Seebach, Actin filament dynamics and endothelial cell junctions: the Ying and Yang between stabilization and motion, Cell. Tissue Res. 355 (2014) 529–543, http://dx.doi.org/10.1007/s00441-014-1856-2.

[19] M.J. Humphries, Cell. Adhes. Assays 18 (2001) 9–13.

[20] D.H. Manicourt, V. Lefebvre, An assay for matrix metalloproteinases and other proteases acting on proteoglycans, casein, or gelatin, Anal. Biochem. 215 (1993) 171–179, http://dx.doi.org/10.1006/abio.1993.1572.

[21] K. Saotome, H. Morita, M. Umeda, Cytotoxicity test with simplified crystal violet staining method using microtitre plates and its application to injection drugs, Toxicol. In Vitro 3 (1989) 317–321, http://dx.doi.org/10.1016/0887-2333(89)90039-8.

[22] B.S. Fogh, H.A. Multhaupt, J.R. Couchman, Protein kinase C, focal adhesions and the regulation of cell migration, HCS 62 (2013) 172–184, http://dx.doi.org/10.1369/0022155413517701.